

## Article

# Effect of Cyanuric Acid as an Efficient Nucleating Agent on the Crystallization of Novel Biodegradable Branched Poly(Ethylene Succinate)

Kangjing Zhang and Zhaobin Qiu \*

State Key Laboratory of Chemical Resource Engineering, Beijing University of Chemical Technology, Beijing 100029, China; 2018400077@grad.buct.edu.cn

\* Correspondence: qiuzb@mail.buct.edu.cn

**Abstract:** Novel biodegradable branched poly(ethylene succinate) (b-PES) composites, i.e., nucleated b-PES samples, were prepared by incorporating low loadings of cyanuric acid (CA) through a solution and casting method to enhance the crystallization rate. As an efficient nucleating agent, CA could remarkably increase the nonisothermal melt crystallization peak temperature, shorten the crystallization half-time, accelerate the overall isothermal melt crystallization, and enhance the nucleation density of b-PES spherulites in the composites. Despite the addition of CA, the crystallization mechanism and crystal structure of b-PES remained unchanged. A possible epitaxial crystallization mechanism may account for the nucleation of b-PES crystals induced by CA.

**Keywords:** Poly(ethylene succinate); cyanuric acid; crystallization; morphology



**Citation:** Zhang, K.; Qiu, Z. Effect of Cyanuric Acid as an Efficient Nucleating Agent on the Crystallization of Novel Biodegradable Branched Poly(Ethylene Succinate). *Macromol* **2021**, *1*, 112–120. <https://doi.org/10.3390/macromol1020009>

Academic Editor: Dimitrios Bikiaris

Received: 1 March 2021

Accepted: 23 March 2021

Published: 7 April 2021

**Publisher's Note:** MDPI stays neutral with regard to jurisdictional claims in published maps and institutional affiliations.



**Copyright:** © 2021 by the authors. Licensee MDPI, Basel, Switzerland. This article is an open access article distributed under the terms and conditions of the Creative Commons Attribution (CC BY) license (<https://creativecommons.org/licenses/by/4.0/>).

## 1. Introduction

Poly(ethylene succinate) (PES) is one of the most promising biodegradable aliphatic polyesters, showing similar physical properties to those of polyethylene and polypropylene [1]. Many researchers have already extensively reported the fundamental studies with regard to PES, including crystal structure, crystallization, morphology, melting behavior, and enzymatic degradation [2–10]. To meet various practical application requirements, some PES-based copolymers have been further designed and synthesized [11–17]. PES may be synthesized from ethylene glycol and succinic acid via a classical two-step melt polycondensation reaction; therefore, some novel PES-based copolymers have been prepared by introducing the third diol or diacid comonomer during the synthesis process. In literature, the synthesis, thermal properties, crystallization, and degradation behavior of some random linear PES-based copolymers have extensively been reported [11–17]. The structure and properties of these novel PES-based copolymers are directly influenced by both the chemical structure and the composition of the novel third comonomer.

It should also be emphasized that the above PES-based copolymers are all linear aliphatic polyesters. Compared with the linear copolymers, branched PES copolymers have seldom received enough attention [18]. The introduction of short or long side chains (branches) usually affects the structure symmetry of the main chain of the homopolymer and causes the depression of thermal properties; consequently, the physical properties of biodegradable polymers, especially the mechanical properties and degradation behavior, may be further adjusted [18–23]. We recently reported the synthesis, thermal properties, mechanical properties, and hydrolytic degradation of novel *n*-octyl branched PES (b-PES) copolymers, which were prepared through the copolymerization of ethylene glycol and succinic acid in the presence of the comonomer of 1, 2-decanediol. The chain branching gradually decreased the glass transition temperature, melting point, and dynamic storage modulus of branched PES copolymers; moreover, they degraded more slowly than linear PES in the alkaline environment [18]. In addition, the chain branching also reduced the

crystallinity and crystallization of b-PES. The slow crystallization rate of b-PES should be enhanced from a polymer processing viewpoint to shorten the processing time; moreover, the increased crystallinity will in turn affect the physical properties, including both mechanical properties and biodegradation, and influence practical application. The utilization of nucleating agent is an efficient way to increase the crystallization rate; however, such study has not been performed till now.

As a small molecule compound, cyanuric acid (CA) is one of the most efficient nucleating agents for some biodegradable polyesters, such as poly(3-hydroxybutyrate), poly(3-hydroxybutyrate-co-3-hydroxyvalerate), poly(3-hydroxybutyrate-co-3-hydroxyhexanoate), poly(L-lactide) (PLLA), poly(butylene adipate), and poly( $\epsilon$ -caprolactone) (PCL) [24–27]. Low loading of CA remarkably increased the nonisothermal melt crystallization peak temperature ( $T_p$ ), nucleation density of spherulites, and overall isothermal melt crystallization rate of the above polyesters, indicating its efficient nucleating agent feature [24–27]. For instance, at a cooling rate of 5 °C/min, 0.3 wt% of CA increased the  $T_p$  of PLLA by 14.3 °C, while 0.2 wt% of CA increased that of PCL by 7.5 °C [25,27].

In this research, b-PES/CA composites were prepared through a solution and casting method at low CA loadings. The crystallization, morphology, and crystal structure of b-PES/CA composites were studied and compared with those of neat b-PES. The aims of this work are as follows: One, to explore whether CA may promote the crystallization of b-PES as an efficient nucleating agent. Two, to discuss the possible nucleation mechanism. From the results, CA is really an efficient nucleating agent for b-PES. From both polymer crystallization and polymer processing viewpoints, this research should be of interest and importance, as a low content of CA can increase the slow crystallization rate and promote the practical application of novel branched b-PES.

## 2. Experimental Section

Through a typical two-stage polymerization method, the random b-PES sample used in this study ( $M_w = 8.8 \times 10^4$  g/mol,  $M_n = 5.9 \times 10^4$  g/mol, 5 mol% 1, 2-decamethylene succinate (DS) unit) was synthesized by our laboratory [18]. CA was bought from Sigma-Aldrich (Shanghai, China) Trading Co., Ltd. The chemical structures of b-PES and CA are illustrated in Figure 1.

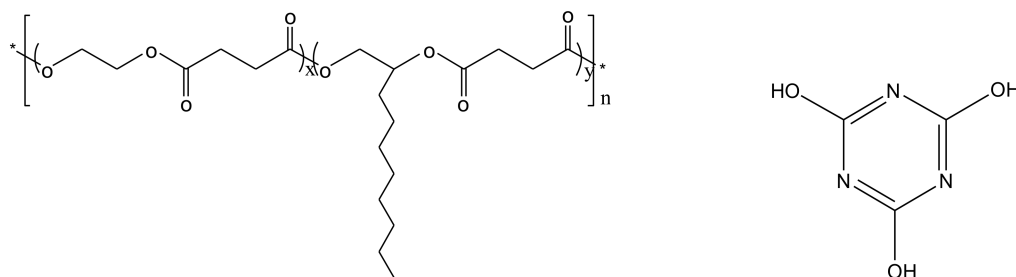


**Figure 1.** Chemical structures of b-PES (left) and CA (right).

The preparation process of the b-PES/CA composites was similar to those of PLLA/CA and PCL/CA composites in literature [25,27]. For simplicity, the composites containing 0.1 and 0.2 wt% CA were abbreviated as b-PES/CA0.1 and b-PES/CA0.2, respectively.

The nonisothermal and isothermal melt crystallization behaviors of neat b-PES and b-PES/CA composites were studied under nitrogen atmosphere with a TA instruments Q100 differential scanning calorimeter (DSC). A fresh sample of about 5 mg was weighed for each test; furthermore, the previous thermal history of the sample was firstly erased by heating to 130 °C and holding there for 3 min to reach the crystal-free melt.

The spherulitic morphologies of neat and nucleated b-PES were observed with a polarizing optical microscope (POM) (Olympus BX51) equipped with a Linkam THMS 600 hot stage.

The crystal structures of neat and nucleated b-PES were investigated at room temperature from 5° to 45° at 5 °/min with a Rigaku D/Max 2500 VB2t/PC X-ray diffractometer at 40 kV and 200 mA.

### 3. Results and Discussion

#### 3.1. Influence of CA on the Nonisothermal and Isothermal Melt Crystallization Behaviors of b-PES

The influence of CA on the nonisothermal and isothermal melt crystallization behaviors of b-PES was studied with DSC under different crystallization conditions. Figure 2 shows the nonisothermal melt crystallization behavior of neat and nucleated b-PES at 5 °C/min. Both neat b-PES and b-PES/CA0.1 presented broad crystallization exothermic peaks, while b-PES/CA0.2 displayed a narrow one. Relative to that of neat b-PES, the crystallization exothermic peaks of b-PES/CA composites shifted upward to higher temperature range, suggesting that low content of CA obviously enhanced the nonisothermal melt crystallization behavior of b-PES. As demonstrated in Figure 2, neat b-PES had a  $T_p$  of 33.4 °C with a crystallization enthalpy ( $\Delta H_c$ ) of 10.7 J/g. For the composites, CA apparently influenced the  $T_p$  and  $\Delta H_c$  values of b-PES. For b-PES/CA0.1,  $T_p$  and  $\Delta H_c$  increased to 43.1 °C and 11.5 J/g, respectively, while they remarkably increased to 52.3 °C and 30.4 J/g, respectively, for b-PES/CA 0.2.

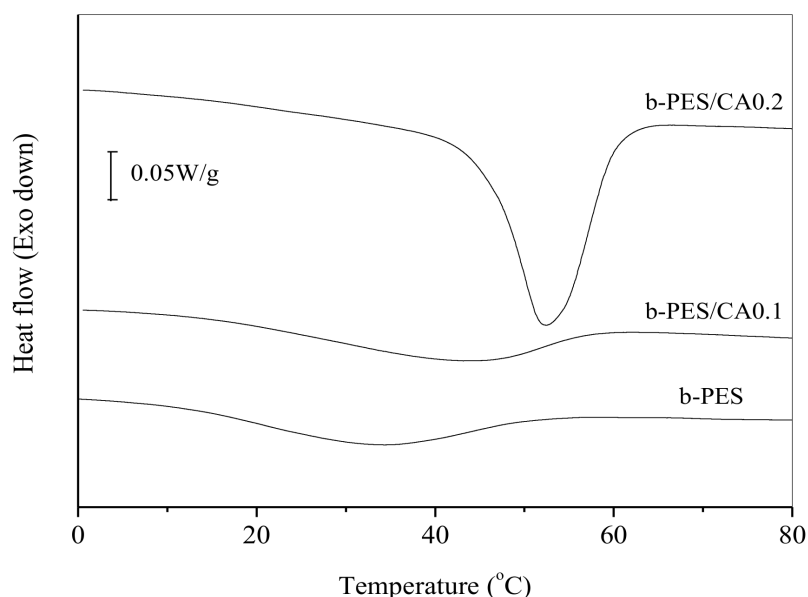


**Figure 2.** Nonisothermal melt crystallization behavior of neat and nucleated b-PES at a cooling rate of 5 °C/min.

The degree of crystallinity ( $X_c$ ) of b-PES was calculated using the follow Equation (1):

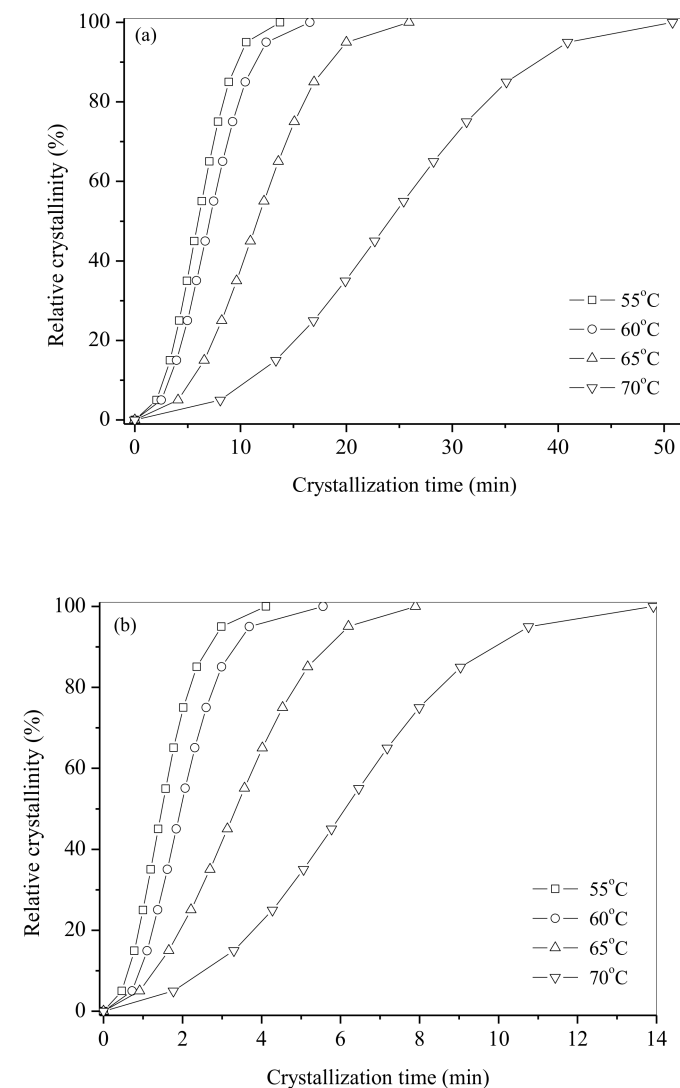
$$X_c = \frac{\Delta H_c}{\phi \Delta H_m^0} \times 100 \% \quad (1)$$

where  $\phi$  is the weight fraction of the b-PES in the composites, and  $\Delta H_m^0$  is the melting enthalpy of a 100% crystalline of b-PES. As the  $\Delta H_m^0$  value of b-PES is not available so far, the  $\Delta H_m^0$  value of PES (180 J/g) was used in this work [28]. By using the above  $\Delta H_c$  values, the  $X_c$  values were calculated to be 6.0%, 6.4%, and 16.9%, respectively, for neat b-PES, b-PES/CA0.1, and b-PES/CA0.2, respectively. All the acquired data are listed in Table 1 for comparison. In brief, the nonisothermal melt crystallization behavior of b-PES was apparently promoted by CA, indicating an efficient nucleating agent effect. In particular, the nonisothermal melt crystallization behavior of b-PES was significantly enhanced at a CA loading of 0.2 wt% as evidenced by the increased  $T_p$ ,  $\Delta H_c$ , and  $X_c$  values in the composite, compared with those of neat b-PES.

**Table 1.** Summary of some parameters of neat and nucleated b-PES during the cooling process.

Samples	b-PES	b-PES/CA0.1	b-PES/CA0.2
$T_p$ (°C)	33.4	43.1	52.3
$\Delta H_c$ (J/g)	10.7	11.5	30.4
$X_c$ (%)	6.0	6.4	16.9

The overall isothermal melt crystallization kinetics of b-PES and its composites was further studied with DSC at different  $T_c$ s ranging from 55 to 70 °C. Figure 3 shows the plots of relative crystallinity versus crystallization time for neat b-PES and b-PES/CA0.2. For simplicity, the plots of b-PES/CA0.1 were not shown here. As illustrated in Figure 3, crystallization time prolonged with increasing crystallization temperature ( $T_c$ ) for both neat b-PES and b-PES/CA0.2, as the nucleation should become difficult at higher  $T_c$  due to the smaller degree of supercooling. At the same  $T_c$ , b-PES/CA 0.2 needed shorter time to complete the isothermal melt crystallization than neat b-PES, indicating that the addition of a low content of CA significantly accelerated the crystallization process of b-PES. For instance, it took neat b-PES about 50 min to complete crystallization at 70 °C, while it only required around 14 min for b-PES/CA 0.2 to finish crystallization at the same  $T_c$ .

**Figure 3.** Plots of relative crystallinity versus crystallization time for (a) neat b-PES and (b) b-PES/CA0.2.

The overall isothermal melt crystallization kinetics of neat b-PES and its composites was further analyzed by the classical Avrami equation, which describes the variation of relative crystallinity ( $X_t$ ) with crystallization time ( $t$ ) as follows in Equation (2):

$$1 - X_t = \exp(-kt^n) \quad (2)$$

where  $k$  is the crystallization rate constant, involving both nucleation and growth rates of the crystals, and  $n$  is the Avrami exponent, relating to crystallization mechanism, i.e., the nucleation type and geometry of the crystals [29,30]. Figure 4 displays the Avrami plots of neat b-PES and b-PES/CA0.2. All the Avrami plots exhibited almost parallel straight lines, demonstrating that the Avrami equation well described the crystallization process of the samples within the studied  $T_c$  range.

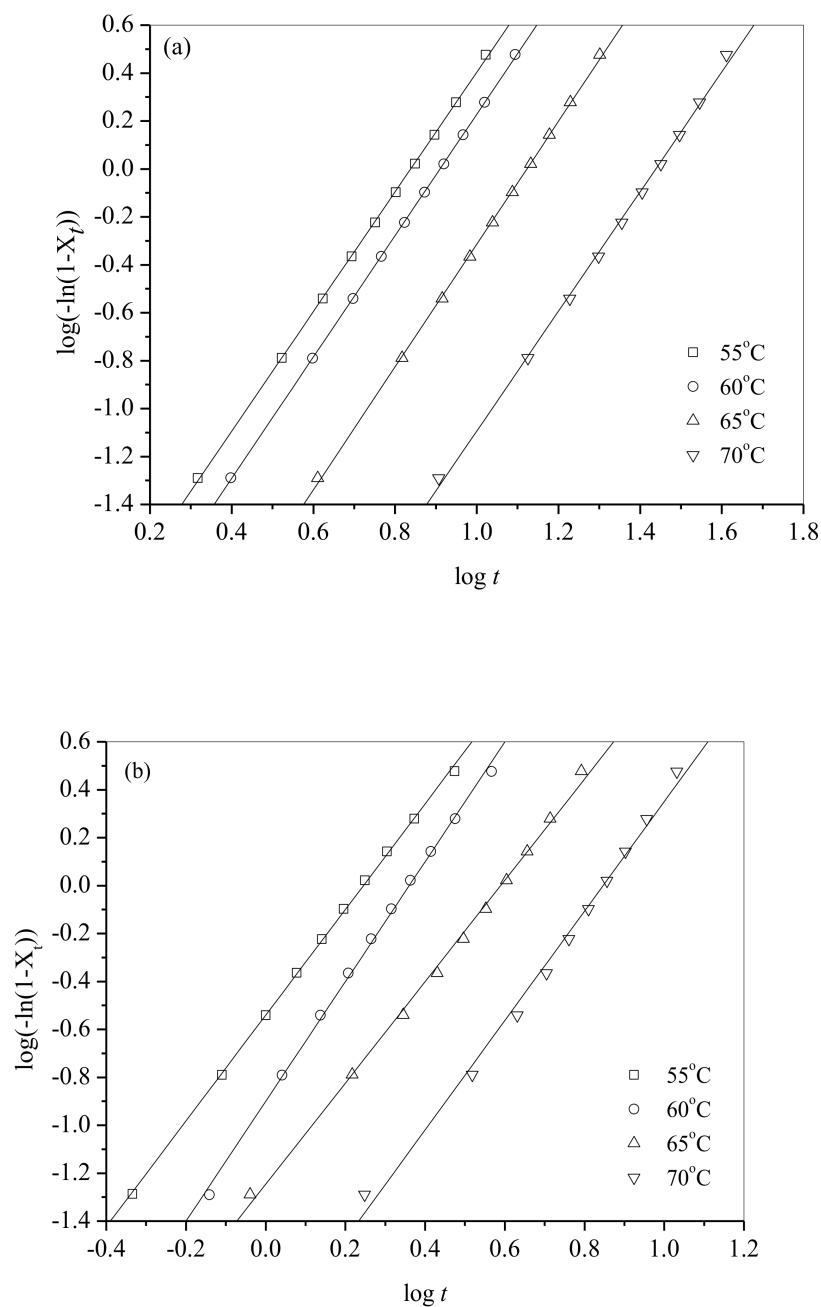


**Figure 4.** Avrami plots for (a) neat b-PES and (b) b-PES/CA0.2.

Table 2 summarizes the  $n$  and  $k$  values of all the three samples within the investigated  $T_c$  range for further comparison. From Table 2, the  $n$  values slightly varied from 1.9 to 2.6, indicating that both neat and nucleated b-PES crystallized through the same crystallization mechanism, regardless of  $T_c$  [31]. In addition, the  $k$  values decreased with an increasing of  $T_c$  for each sample. Through the following equation, crystallization half-time ( $t_{0.5}$ ) was calculated in Equation (3):

$$t_{0.5} = (\ln 2/k)^{1/n} \quad (3)$$

**Table 2.** Summary of the Avrami parameters of neat and nucleated b-PES during the isothermal melt crystallization.

	$T_c$ (°C)	$n$	$k$ (min <sup>-n</sup> )	$t_{0.5}$ (min)
Neat b-PES	55	2.5	$8.07 \times 10^{-3}$	5.94
	60	2.5	$4.97 \times 10^{-3}$	7.21
	65	2.6	$1.33 \times 10^{-3}$	11.08
	70	2.5	$2.57 \times 10^{-4}$	23.58
b-PES/CA0.1	55	1.9	$2.92 \times 10^{-1}$	1.58
	60	2.0	$1.61 \times 10^{-1}$	2.08
	65	2.1	$4.72 \times 10^{-2}$	3.59
	70	1.9	$2.15 \times 10^{-2}$	6.22
b-PES/CA0.2	55	2.2	$2.88 \times 10^{-1}$	1.49
	60	2.5	$1.26 \times 10^{-1}$	1.98
	65	2.1	$5.62 \times 10^{-2}$	3.31
	70	2.3	$1.17 \times 10^{-2}$	5.89

The calculated  $t_{0.5}$  values are also listed in Table 2 for comparison. For each sample,  $t_{0.5}$  obviously increased with increasing  $T_c$ , suggesting slower crystallization rate at higher  $T_c$ . At the same  $T_c$ ,  $t_{0.5}$  significantly decreased with an increase in CA content, indicating that CA accelerated the isothermal melt crystallization process of b-PES in the composites. Moreover,  $t_{0.5}$  of b-PES/CA 0.2 was slightly smaller than that of b-PES/CA 0.1 at the same  $T_c$ , revealing that the effect of CA on the enhanced crystallization rate of b-PES leveled off when the loading was up to 0.2%. Figure 5 displays the plots of  $1/t_{0.5}$  versus  $T_c$  for neat b-PES and its composites. The greater  $1/t_{0.5}$ , the faster crystallization rate. As clearly depicted in Figure 5,  $1/t_{0.5}$  gradually decreased with the increase of  $T_c$  for neat and nucleated b-PES. At a given  $T_c$ , the  $1/t_{0.5}$  values of nucleated b-PES were always obviously greater than that of neat b-PES, demonstrating the accelerated crystallization process of b-PES induced by the presence of CA. The plots of b-PES/CA0.1 and b-PES/CA0.2 were close to each other; moreover, the plot of b-PES/CA0.2 was only slightly higher than that of b-PES/CA0.1, suggesting that the nucleation effect of CA may reach saturation in b-PES/CA 0.2.

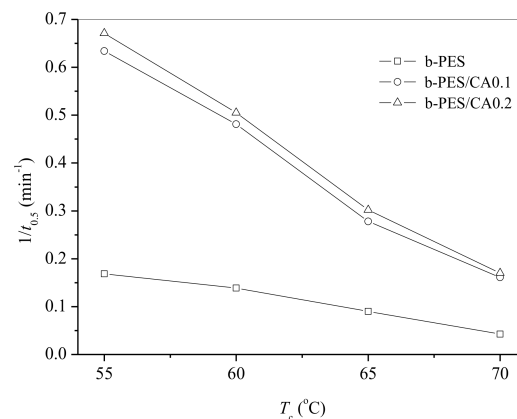


**Figure 5.** Variations of  $1/t_{0.5}$  with  $T_c$  for neat and nucleated b-PES.

### 3.2. Spherulitic Morphology and Crystal Structure Studies of Neat and Nucleated b-PES

To provide direct evidence of the nucleating agent effect of CA, the spherulitic morphology of neat b-PES and its composites was studied in this section with POM. Figure 6 displays the spherulites of neat and nucleated b-PES after completely crystallizing at 60 °C. For both neat b-PES and its composites, quite a number of spherulites were observed. Compared with that of neat b-PES, CA significantly decreased the size of b-PES spherulites and increased the number of spherulites in the composites, thereby increasing the nucleation density of b-PES spherulites. However, the difference in the size and number of b-PES spherulites seemed not so big on increasing the CA loading from 0.1 to 0.2%, suggesting again that the nucleation effect tended to level off.

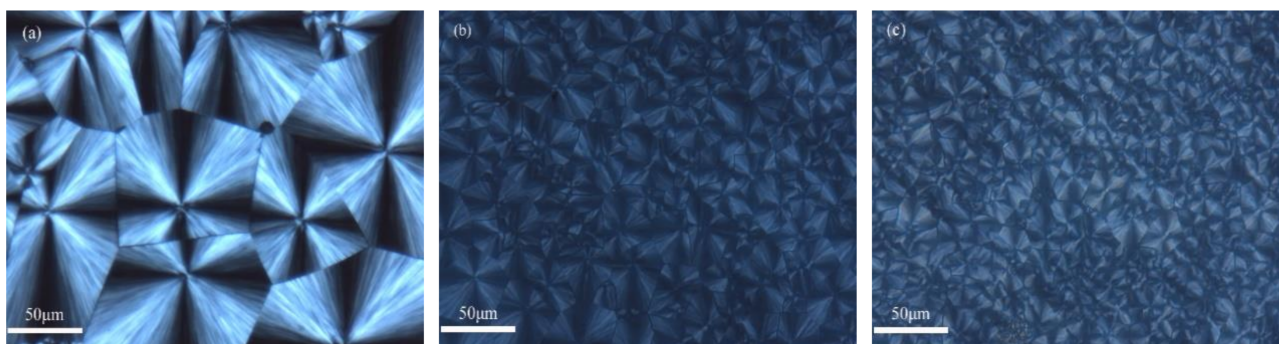


**Figure 6.** Spherulites of (a) neat b-PES, (b) b-PES/CA0.1 and (c) b-PES/CA0.2 after isothermal melt crystallization at 60 °C.

The effect of CA on the crystal structure of b-PES was further investigated. Figure 7 shows the wide angle X-ray diffraction (WAXD) profiles of neat and nucleated b-PES after isothermally crystallizing at 60 °C for 72 h. As clearly shown in Figure 7, all samples showed similar WAXD profiles, suggesting that CA did not change the crystal structure of b-PES. For neat b-PES, two main diffraction peaks appeared at 19.60° and 22.67°, corresponding to planes (021) and (200) of b-PES crystals, respectively [1]. For b-PES/CA0.1, the two diffraction peaks were observed at 20.10° and 23.23°, respectively. For b-PES/CA0.2, they appeared at  $2\theta = 20.22^\circ$  and 23.35°, respectively. With increasing CA loading, the two diffraction peaks slightly shifted upward to a higher  $2\theta$  range, suggesting the variation in unit cell parameters. In brief, the incorporation of CA did not change the crystal structure of b-PES, despite the slight variation in unit cell parameters.

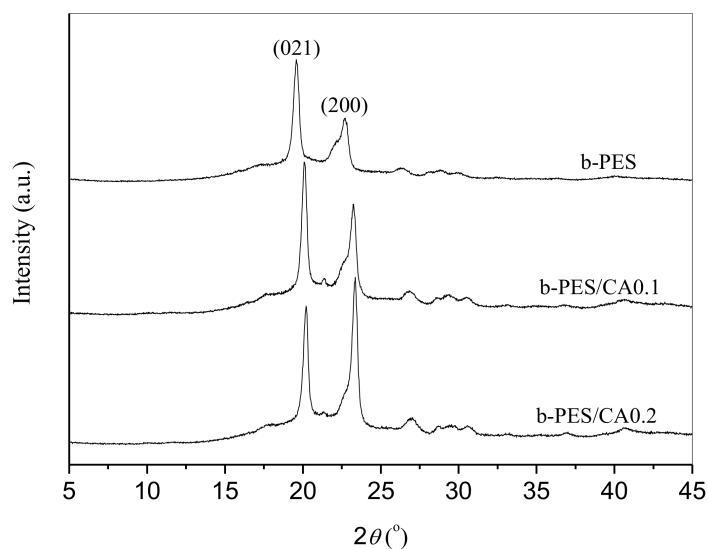


**Figure 7.** WAXD patterns of neat and nucleated b-PES after crystallizing at 60 °C.

Based on the above results, only a small amount of CA significantly enhanced the crystallization rate of b-PES by acting as an efficient nucleating agent. From both polymer crystallization and practical application viewpoints, the nucleation mechanism of b-PES induced by CA was further discussed. So far, the exact nucleation mechanism is still uncertain. One possible nucleation mechanism was proposed based on the crystal structures of b-PES and CA. The crystal structure of b-PES was an orthorhombic unit cell with lattice parameters of  $a = 0.760$  nm,  $b = 1.075$  nm, and  $c = 0.833$  nm [2], while a monoclinic unit cell with lattice parameters of  $a = 0.775$  nm,  $b = 0.674$  nm,  $c = 1.191$  nm, and  $\beta = 130.7^\circ$  was determined for that of CA [32]. The  $a$  values of both b-PES and CA were close to each other; consequently, the mismatching was smaller than 2%. Therefore, b-PES crystals probably grow on the surface of CA crystals via a possible epitaxial crystallization mechanism, which needs further investigation [22–25].

#### 4. Conclusions

The effect of CA on the significantly enhanced crystallization rate of novel branched biodegradable b-PES as an efficient nucleating agent was studied for the first time in this research. Through a solution and casting method, b-PES/CA composites, i.e., nucleated b-PES samples, were prepared at low CA loadings. During the nonisothermal melt crystallization, CA obviously increased the nonisothermal melt crystallization peak temperature; therefore, the nonisothermal melt crystallization behavior of b-PES was remarkably enhanced in the composites. CA significantly increased the isothermal crystallization rate of b-PES but did not change the crystallization mechanism. The increase in CA loading from 0.1 to 0.2% did not apparently further increase the crystallization rate of b-PES, indicating that the enhancement effect tended to level off. The spherulitic morphology study directly confirmed the nucleating agent effect of CA, as the nucleation density of b-PES spherulites increased significantly in the composites. In the composites, CA did not change the crystal structure of b-PES despite the slight variation of the lattice parameters. Based on the crystal structures of b-PES and CA, the nucleation of b-PES crystals induced by CA was discussed via a possible epitaxial crystallization mechanism. The practical application of novel biodegradable b-PES may be promoted by CA as an effective nucleating agent from the viewpoints of polymer processing and polymer crystallization.

**Author Contributions:** Investigation, writing—original draft preparation, K.Z.; supervision, writing—review and editing, Z.Q. Both the authors have read and agreed to the published version of the manuscript.

**Funding:** This research received no external funding.

**Institutional Review Board Statement:** Not applicable.

**Informed Consent Statement:** Not applicable.

**Data Availability Statement:** The data presented in this study are available on request from the corresponding author.

**Conflicts of Interest:** The authors declare no conflict of interest.

#### References

1. Fujimaki, T. Processability and Properties of Aliphatic Polyesters, 'BIONOLLE', Synthesized by Polycondensation Reaction. *Polym. Degrad. Stab.* **1998**, *59*, 209–214. [[CrossRef](#)]
2. Ueda, A.; Chatani, Y.; Tadokoro, H. Structure Studies of Polyesters. IV. Molecular and Crystal Structure of Poly(ethylene succinate) and Poly(ethylene oxalate). *Polym. J.* **1971**, *2*, 387–397. [[CrossRef](#)]
3. Gan, Z.; Abe, H.; Doi, Y. Biodegradable Poly(ethylene succinate) (PES). 1. Crystal Growth Kinetics and Morphology. *Biomacromolecules* **2000**, *1*, 704–712. [[CrossRef](#)] [[PubMed](#)]
4. Gan, Z.; Abe, H.; Doi, Y. Biodegradable Poly(ethylene succinate) (PES). 2. Crystal Morphology of Melt-crystallized Ultrathin film and Its Change after Enzymatic Degradation. *Biomacromolecules* **2000**, *1*, 713–720. [[CrossRef](#)]
5. Qiu, Z.; Ikehara, T.; Nishi, T. Crystallization Behavior of Biodegradable Poly(ethylene succinate) from the Amorphous State. *Polymer* **2003**, *44*, 5429–5437. [[CrossRef](#)]

6. Qiu, Z.; Fujinami, S.; Komura, M.; Nakajima, K.; Ikehara, T.; Nishi, T. Nonisothermal Crystallization Kinetics of Poly(butylene succinate) and Poly(ethylene succinate). *Polym. J.* **2004**, *36*, 642–646. [[CrossRef](#)]
7. Papageorgiou, G.; Bikiaris, D.; Achilias, D. Effect of Molecular Weight on the Cold-crystallization of Biodegradable Poly(ethylene succinate). *Thermochim. Acta* **2007**, *457*, 41–54. [[CrossRef](#)]
8. Qiu, Z.; Komura, M.; Ikehara, T.; Nishi, T. DSC and TMDSC study of Melting Behavior of Poly(butylene succinate) and Poly(ethylene succinate). *Polymer* **2003**, *44*, 7781–7785. [[CrossRef](#)]
9. Iwata, T.; Doi, Y.; Isono, K.; Yoshida, Y. Morphology and Enzymatic Degradation of Solution-grown Single Crystals of Poly(ethylene succinate). *Macromolecules* **2001**, *34*, 7343–7348. [[CrossRef](#)]
10. Tezuka, Y.; Ishii, N.; Kasuya, K.; Mitomo, H. Degradation of Poly(ethylene succinate) by Mesophilic Bacteria. *Polym. Degrad. Stab.* **2004**, *84*, 115–121. [[CrossRef](#)]
11. Papageorgiou, G.; Bikiaris, D. Synthesis and Properties of Novel Biodegradable/Biocompatible Poly[propyleneco-(ethylene succinate)] Random Copolyesters. *Macromol. Chem. Phys.* **2009**, *210*, 1408–1421. [[CrossRef](#)]
12. Yang, Y.; Qiu, Z. Crystallization and Melting Behavior of Biodegradable Poly(ethylene succinate-co-6mol% butylene succinate). *J. Appl. Polym. Sci.* **2011**, *122*, 105–111. [[CrossRef](#)]
13. Li, X.; Qiu, Z. Crystallization Kinetics, Morphology, and Mechanical Properties of Novel Poly(ethylene succinate-co-octamethylene succinate). *Polym. Test.* **2015**, *48*, 125–132. [[CrossRef](#)]
14. Li, X.; Qiu, Z. Synthesis and Properties of Novel Poly(ethylene succinate-co-decamethylene succinate) Copolymers. *RSC Adv.* **2015**, *5*, 103713–103721. [[CrossRef](#)]
15. Wu, H.; Qiu, Z. Synthesis, Crystallization Kinetics and Morphology of Novel Poly(ethylene succinate-co-ethylene adipate) Copolymers. *CrystEngComm* **2012**, *14*, 3586–3595. [[CrossRef](#)]
16. Qiu, S.; Su, Z.; Qiu, Z. Crystallization Kinetics, Morphology, and Mechanical Properties of Novel Biodegradable Poly(ethylene succinate-co-ethylene suberate) Copolyesters. *Ind. Eng. Chem. Res.* **2016**, *55*, 10286–10293. [[CrossRef](#)]
17. Qiu, S.; Su, Z.; Qiu, Z. Isothermal and Nonisothermal Crystallization Kinetics of Novel Biobased Poly(ethylene succinate-co-ethylene sebacate) Copolymers from the Amorphous State. *J. Therm. Anal. Calorim.* **2017**, *129*, 801–808. [[CrossRef](#)]
18. Qiu, S.; Zhang, K.; Su, Z.; Qiu, Z. Thermal Behavior, Mechanical and Rheological Properties, and Hydrolytic Degradation of Novel Branched Biodegradable Poly(ethylene succinate) Copolymers. *Polym. Test.* **2018**, *66*, 64–69. [[CrossRef](#)]
19. Kim, M.; Kim, K.; Jin, H.; Park, J.; Yoon, J. Biodegradability of Ethyl and *n*-octyl Branched Poly(ethylene adipate) and Poly(butylene succinate). *Eur. Polym. J.* **2001**, *37*, 1843–1847. [[CrossRef](#)]
20. Kim, E.; Bae, J.; Im, S.; Kim, B.; Han, Y. Preparation and Properties of Branched Polybutylenesuccinate. *J. Appl. Polym. Sci.* **2001**, *80*, 1388–1394. [[CrossRef](#)]
21. Jin, H.; Kim, D.; Kim, M.; Lee, I.; Lee, H.; Yoon, J. Synthesis and Properties of Poly(butylene succinate) with *n*-hexenyl Side Branches. *J. Appl. Polym. Sci.* **2001**, *81*, 2219–2226. [[CrossRef](#)]
22. Chae, H.; Park, S.; Kim, B.; Kim, D. Effect of Methyl Substitution of the Ethylene Unit on the Physical Properties of Poly(butylene succinate). *J. Polym. Sci. Polym. Phys.* **2004**, *42*, 1759–1766. [[CrossRef](#)]
23. Wang, G.; Gao, B.; Ye, H.; Xu, J.; Guo, B. Synthesis and Characterizations of Branched Poly(butylene succinate) Copolymers with 1,2-octanediol Segments. *J. Appl. Polym. Sci.* **2010**, *117*, 2538–2544. [[CrossRef](#)]
24. Pan, P.; Shan, G.; Bao, Y.; Weng, Z. Crystallization Kinetics of Bacterial Poly(3-hydroxybutyrate) Copolyesters with Cyanuric Acid as A Nucleating Agent. *J. Appl. Polym. Sci.* **2013**, *129*, 1374–1382. [[CrossRef](#)]
25. Weng, M.; Qiu, Z. Effect of Cyanuric Acid on The Crystallization Kinetics and Morphology of Biodegradable Poly(L-lactide) as an Efficient Nucleating Agent. *Thermochimi. Acta* **2014**, *577*, 41–45. [[CrossRef](#)]
26. Yang, J.; Chen, Y.; Qin, S.; Liu, J.; Bi, C.; Liang, R.; Dong, T.; Feng, X. Effects of Cyanuric Acid on Crystallization Behavior, Polymorphism, and Phase Transition of Poly(butylene adipate). *Ind. Eng. Chem. Res.* **2015**, *54*, 8048. [[CrossRef](#)]
27. Zhang, K.; Qiu, Z. Enhanced Crystallization Rate of Biodegradable Poly( $\epsilon$ -caprolactone) by Cyanuric Acid as an Efficient Nucleating Agent. *Chin. J. Polym. Sci.* **2017**, *35*, 1517–1523. [[CrossRef](#)]
28. Papageorgiou, G.; Bikiaris, D. Crystallization and Melting Behavior of Three Biodegradable Poly(alkylene succinates). A Comparative Study. *Polymer* **2005**, *46*, 12081–12092. [[CrossRef](#)]
29. Avrami, M. Kinetics of Phase Change. II Transformation-time Relations for Random Distribution of Nuclei. *J. Chem. Phys.* **1940**, *8*, 212–224. [[CrossRef](#)]
30. Avrami, M. Granulation, Phase Change, and Microstructure Kinetics of Phase Change. III. *J. Chem. Phys.* **1941**, *9*, 177–184. [[CrossRef](#)]
31. Wunderlich, B. *Macromolecular Physics*; Academic Press: New York, NY, USA, 1976.
32. Verschoor, G.; Keulen, E. Electron Density Distribution in Cyanuric Acid. I. An X-ray Diffraction Study at Low Temperature. *Acta Cryst.* **1971**, *B27*, 134–145. [[CrossRef](#)]